JOURNAL OF CATALYSIS **173,** 490–500 (1998)
ARTICLE NO. CA971952

Side-Chain Alkylation of Toluene with Methanol over Alkali-Exchanged Zeolites X, Y, L, and β

Wendi S. Wieland,*[,1] Robert J. Davis,*[,2] and Juan M. Garces†

*Department of Chemical Engineering, University of Virginia, Charlottesville, Virginia 22903-2442; and †Dow Chemical Company, Catalysis R&D, 1776 Building, Midland, Michigan 48674

Received July 15, 1997; revised October 23, 1997; accepted October 24, 1997

Alkali-exchanged zeolites (X, Y, L, and β) and alkali-impregnated mesoporous alumina were studied as catalysts for toluene alkylation with methanol. The effects of zeolite basicity, zeolite particle size, and pore dimensionality were examined. At 680–690 K and atmospheric pressure, highly basic, alkali-exchanged zeolites X and Y were active for toluene alkylation but primarily decomposed methanol to carbon monoxide. Cesium-exchanged zeolites L and β were also active alkylation catalysts but required higher temperatures to attain similar aromatic yields. More importantly, very little carbon monoxide was produced over the L and β catalysts. Reactivity results for a ball-milled Y zeolite suggested that variations in particle size did not account for the observed differences in methanol decomposition over the catalysts. Infrared spectroscopy and thermogravimetric analysis indicated that alkali-exchanged X and Y zeolites adsorbed orders of magnitude greater amounts of CO_2 than CsL and Csβ zeolites. Apparently, zeolites with low base site densities and appropriate base strengths selectively alkylate toluene without decomposing methanol to carbon monoxide. The observed activities of L, β, X, and Y demonstrate that zeolites with one-, two-, and three-dimensional pore networks catalyze side-chain alkylation. Mesoporous alumina modified with cesium and boron was inactive for toluene alkylation but decomposed methanol to carbon monoxide. The inactivity of a basic, mesoporous alumina for conversion of toluene suggests that physical constraints and proximity of acid/base sites within molecular sieve environments may facilitate the side-chain alkylation reaction. © 1998 Academic Press

Key Words: **toluene; methanol; styrene; ethylbenzene; formaldehyde; zeolite; alumina; potassium; cesium; boron.**

INTRODUCTION

Alkylation of toluene with methanol over solid bases is an attractive synthetic route to styrene and ethylbenzene compared to the traditional Friedel–Crafts alkylation of benzene with ethylene. Even though side-chain alkylation of toluene has been known for several decades (1), the nature of the catalyst and the identity of the base site remain elusive. Alkali-exchanged zeolites have demonstrated the highest activities and selectivities for toluene alkylation with methanol and have been the focus of most works in the area. It is generally believed that formaldehyde, formed *in situ* from methanol dehydrogenation, is the actual alkylating reagent. Indeed, formaldehyde is more reactive than methanol for toluene alkylation over basic zeolites (2). Also, surface formates have been observed by NMR spectroscopy (3) and IR spectroscopy (4, 5) on alkali-exchanged zeolites after exposure to methanol. The major side reaction during toluene alkylation over solid bases is the formation of carbon monoxide from decomposition of the alkylating agent. Thus, materials that catalyze toluene alkylation without methanol decomposition would be highly desirable.

Unland and Barker reported that incorporation of boron and phosphorous promoters onto alkali-exchanged zeolites X and Y led to increased aromatic selectivities, regardless of the form of the precursor or method of addition (6). In a subsequent paper, they suggested that the effect of adding boron was to neutralize some of the strongly basic sites that catalyze rupture of CH bonds in methanol (7).

If formation of formaldehyde from methanol *in situ* is critical to the alkylation reaction, then addition of a dehydrogenating agent to the zeolite catalysts may be beneficial. To test that idea, Lacroix *et al.* prepared catalysts from Cs-exchanged X zeolites by addition of Cu and Ag (8). The presence of those metals (and boron) on CsX substantially improved the alkylation yield over an unpromoted catalyst. However, most of their experiments used H_2 as the carrier gas.

Post-exchange treatment of zeolites has also been used to modify basic properties. For example, Engelhardt *et al.* found that washing KX zeolites with water resulted in materials that catalyzed formation of styrene, ethylbenzene and xylenes (9). Additional washes caused xylene formation to increase at the expense of side-chain alkylation. Washing alkali-exchanged zeolites with water apparently introduces some acidity into the catalysts. In contast, post-exchange treatment of KX zeolite with KOH solution

[1] Present address: Engelhard Corporation, 25 Middlesex Essex Turnpike, Iselin, NJ 08830.

[2] To whom correspondence should be addressed.

0021-9517/98 $25.00

completely suppressed xylene formation and promoted side-chain alkylation. Occluded KOH appears to play an important role in the base-catalyzed reaction. Likewise, Hathaway and Davis showed that occlusion of cesium oxide into the pores of Cs-exchanged X and Y zeolites, via acetate impregnation and decomposition, promoted the reaction of toluene and methanol (10). Unfortunately, substantial amounts of methanol decompose to carbon monoxide over such strongly basic materials.

Theoretical and experimental works by Itoh *et al.* describe the cooperation of Lewis acid/base pairs in the mechanism of toluene alkylation (11, 12). A base site activates the methyl group of toluene, whereas the acid site interacts with the aromatic ring. Consistent with the proposed synergism between acid and base sites, small amounts of Li added to RbX catalysts significantly promoted the alkylation reaction. However, Palomares *et al.* found that the sorption strength of toluene increased with increasing cation size, presumably due to a better steric match of the π orbitals of toluene to the alkali (13).

Alkali-loaded activated carbons also catalyze the toluene alkylation reaction, which demonstrates that zeolite frameworks are not required for the reaction (14). For example, a cesium-loaded, boron-promoted carbon was as active as Cs-exchanged X zeolite for toluene alkylation (14). In that work, the authors suggested that alkali oxides and alkali metal vapors may constitute the basic sites needed for activation of toluene.

Wang *et al.* found that a mixture of KX and KZSM-5 zeolites was more active than the separate components (15). They proposed that the strong base sites of the KX component activate the side-chain of toluene and that the weak base sites of the smaller pore KZSM-5 catalyze methanol conversion to formaldehyde.

Clearly, the side-chain alkylation of toluene is affected by the basic character of the catalysts. However, the porosity of the catalysts may also play a critical role in the reaction since nearly all of the active catalysts studied to date are microporous. This paper presents results from catalyst characterization and toluene alkylation over a variety of alkali-exchanged zeolites having various Si/Al ratios, boron loadings, particle sizes and pore networks. Characterization methods include elemental analysis, scanning electron microscopy, Ar physisorption, X-ray diffraction, CO_2 chemisorption and IR spectroscopy. A nonmicroporous alumina impregnated with Cs and B is also evaluated as a potential alkylation catalyst.

EXPERIMENTAL METHODS

Catalyst Synthesis

Zeolites X and Y, obtained from Union Carbide Corporation in the sodium form, were ion exchanged with aqueous solutions of alkali salts (Aldrich: cesium acetate, 99.9%; potassium acetate, 99%) according to conventional exchange procedures. This typically involved triple exchange in 1.0 M aqueous solutions of alkali acetate at ambient temperature. Since washing of zeolites with pure water can partially remove alkali ions, the exchanged zeolites were rinsed with dilute hydroxide solutions. The appropriate hydroxide (Aldrich: cesium hydroxide, 99.9% in a 50 wt% aqueous solution; potassium hydroxide, 85%) was dissolved in enough water to give the rinse solution a pH of 13.3. The materials were then dried in air at 373 K overnight. Some alkali-exchanged zeolites were modified with boric acid (Aldrich, 99.99%) using standard incipient wetness impregnation. Catalysts were pretreated at 783 K in flowing helium for 2 h prior to reaction. Previous work in our lab showed that bulk alkali acetate decomposed in He at temperatures less than 773 K (16). Indeed, no acetate bands were observed in the IR spectra of our pretreated samples.

Zeolite L (obtained from Union Carbide Corp. in a potassium-rich form) was initially exchanged twice in a 0.1 M aqueous solution of ammonium nitrate at room temperature. The zeolite was washed between ammonium exchanges but not calcined. To incorporate cesium, the sample was exchanged three times in 0.1 M aqueous solutions of cesium acetate. This catalyst was also pretreated at 783 K in flowing helium for 2 h prior to reaction.

Zeolite β (obtained from PQ Corporation) was exchanged three times in 0.1 M aqueous solutions of cesium acetate and pretreated at 783 K in flowing helium for 2 h prior to reaction.

Mesoporous alumina was synthesized according to the method described by Vaudry *et al.* (17) using n-propanol and lauric acid. The synthesis mixture was aged for 24 h and then heated to 383 K for 48 h. The resulting mesoporous alumina was filtered, rinsed in distilled deionized water, rinsed in absolute ethanol (AAPER, 95%), and dried at room temperature. To remove the surfactant, the material was calcined in flowing air at 773 K for 4 h. Cesium was incorporated onto mesoporous alumina by the method of incipient wetness impregnation. The cesium-modified mesoporous alumina was dried in air at 373 K overnight. Boron, in the initial form of boric acid (Aldrich, 99.99%), was also incorporated using incipient wetness impregnation. The modified aluminas were pretreated *in situ* at 783 K in flowing helium for 2 h prior to reaction.

The particle size of micron scale zeolite NaY from Union Carbide Corporation was reduced using a dry ball milling method to produce submicron scale particles. A Spex 8000 Mixer/Mill was used with a zirconia vial and zirconia mixing ball. Typically, the milled zeolite was washed in aqueous 0.05 M sodium hydroxide solution at 353 K for 2 h. Following the hydroxide wash, milled particles were allowed to settle for 30 min. The remaining solution was decanted and allowed to sit for 6 h. The colloidal solution remaining after 6 h was discarded and the settled particles were dried

overnight in air at 373 K. This milled sample of zeolite Y was then exchanged twice with 0.10 M aqueous solutions of ammonium nitrate. To incorporate cesium, the sample was subsequently exchanged once in a 0.3 M aqueous cesium acetate solution and twice in 0.1 M aqueous cesium acetate solutions. The catalyst was then pretreated at 783 K in flowing helium for 2 h prior to reaction.

Catalyst Characterization

Flame emission spectroscopy, performed by Galbraith Laboratories, Inc. (Knoxville, TN), was used to determine elemental compositions. Particle sizes were determined by inspection of scanning electron micrographs (JEOL JXA-840 Electron Probe Microanalyzer). Argon adsorption isotherms were measured at liquid Ar temperature with an Omnisorp 100CX (Coulter Corporation) automated adsorption system in the continuous flow mode of operation. Micropore volumes of the zeolites were calculated from the Ar adsorption isotherms. X-ray powder diffraction was used to examine the crystallinity of the catalysts. Diffraction patterns were collected at 1° min^{-1} on a Scintag diffractometer with a CuKα X-ray source. Thermogravimetric analyses were performed on a TA Instruments TGA 2050 system. Typically, the catalyst powder was heated in ultrahigh purity helium (BOC Gases, 99.999%) at a rate of 3 K min^{-1} to a final temperature of 773 K and held isothermally for 2 h. Next, the temperature was reduced to 373 K at a rate of 6 K min^{-1} and held isothermally for 30 min. Ultrahigh purity carbon dioxide (BOC, 99.999%), mixed with the helium purge gas, contacted the sample for 30 min. After adsorption at 373 K, the sample was purged in helium for 1 h to remove weakly adsorbed carbon dioxide. Fourier transform infrared spectroscopy was performed using a Bio-Rad FTS 60A spectrometer. Catalyst powder was pressed, without binder, into a thin pellet of approximately 10 mm in diameter. A quartz IR cell fitted with KBr windows and a sapphire pellet holder was used for *in situ* measurements. Catalyst pellets were heated in flowing helium (BOC, 99.999%) to 773 K at 5 K min^{-1} and held isothermally for 18 h. The pellet was then cooled from 773 K at a rate of 5 K min^{-1} to the scanning temperature. Trace amounts of water were removed from the purge gas by passage through a bed of 3A molecular sieves (Davison Chemical) and a cold trap immersed in a dry ice–acetone bath. The spectra were averaged over 256 scans collected at a resolution of 2 cm^{-1}.

Catalytic Reaction

Catalyst powders were pressed, crushed, and sieved to −4/+60 mesh, and loaded into a single pass, quartz, fixed bed reactor. The temperature of the reactor was increased from room temperature to 783 K at a rate of 5 K min^{-1} in flowing helium (BOC gases, 99.999%) and remained at that value for 1 h before cooling to the reaction temperature. While the catalyst cooled, a liquid mixture of toluene (Aldrich, 99.8%) and methanol (Mallinckrodt, 99.9%) having a 5 : 1 molar ratio was pumped at a rate of 1.0–2.0 ml h^{-1} and vaporized into a flowing helium stream that bypassed the reactor. After flow rates and temperatures were stabilized, the reactant stream of helium and organics (5 : 1 molar ratio of He to organics) was fed to the reactor at a typical rate of 2160 ml h^{-1} (STP). Two thermocouples, one located in the catalyst bed and one on the outer wall of the reactor, were used to monitor the reaction temperature. Typically, a temperature difference of 10–20 K was observed between the two thermocouples. The temperatures reported here are an average of the two readings. The effluent from the reactor was analyzed by gas chromatography. Prior to sampling, a known flowrate of methane (BOC, 99.999%) was blended into the effluent stream. The heavy components in the effluent (toluene, methanol, styrene, and ethylbenzene) were analyzed with a 0.53-mm × 50-m, HP1 fused silica capillary column connected to a flame ionization detector (FID). A Haysep Q (−80/+100 mesh), 10 ft, stainless steel packed column connected to a thermal conductivity detector (TCD) was used to analyze for carbon monoxide and carbon dioxide. However, carbon dioxide was never detected in significant amounts. Heavy components were condensed in an ice-cooled trap before the light gases were injected onto the second column. Methane was detected by both the FID and TCD and served as an effective internal standard for both light and heavy components.

The reactivity results are presented as methanol conversion, aromatic yield, and aromatic selectivity, which are defined as follows (quantities are molar flowrates):

$$\text{methanol conversion} = 1 - \frac{\text{MeOH}_{\text{exit}}}{\text{MeOH}_{\text{feed}}}$$

$$\text{aromatic yield} = \frac{\text{S} + \text{EB}}{\text{MeOH}_{\text{feed}}}$$

$$\text{aromatic selectivity} = \frac{\text{S} + \text{EB}}{\text{S} + \text{EB} + \text{CO}},$$

where MeOH, S, and EB represent methanol, styrene, and ethylbenzene, respectively.

RESULTS

A summary of the results from elemental analyses and argon adsorption studies of the zeolite catalysts is reported in Table 1. For faujasite-type zeolites, the unit cell composition was based on 384 oxygen atoms per unit cell. Zeolites L and β were assumed to have 72 and 128 oxygen atoms per unit cell, respectively. Deviations from ideal unit cell compositions most likely result from small errors in elemental analysis and noncrystalline phases in the samples. The micropore volume is calculated from the total uptake of Ar at a relative pressure of 0.3 and subsequent conversion to a liquid volume. As shown in Table 1, the micropore volume

TABLE 1

Elemental Analyses and Pore Volumes of Zeolite Catalysts

Catalyst	Composition	Si/Al	Pore volume/cm^3 Ar (g)$^{-1}$	Pore volume/cm^3 Ar (g zeolite framework[a])$^{-1}$
NaX	$Na_{78.8}Si_{104}Al_{87.7}O_{384}$	1.19	0.239	0.277
KX	$K_{66.6}Na_{13.6}Si_{104}Al_{88.1}O_{384}$	1.18	0.199	0.250
CsX	$Cs_{51.9}Na_{28.3}Si_{110}Al_{81.7}O_{384}$	1.35	0.122	0.198
NaY	$Na_{53.7}Si_{138}Al_{54.1}O_{384}$	2.56	0.254	0.281
CsY	$Cs_{48.5}Na_{8.50}Si_{140}Al_{52.3}O_{384}$	2.68	0.102	0.163
Csβ	$Cs_{9.55}Na_{0.043}Si_{59.1}Al_{4.81}O_{128}$	12.3	0.162	0.216
CsL	$Cs_{4.08}K_{3.99}Si_{27.1}Al_{8.80}O_{72}$	3.08	0.068	0.090

[a] Zeolite framework consists of silicon and aluminum oxides on a cation-free basis.

per gram of zeolite decreased after exchange of heavy alkali, which is consistent with the larger size and the greater atomic weight of the exchanged cation. Even when the effect of cation atomic weight is eliminated in the calculation, a decrease in pore volume with exchange of heavy alkali is still observed. The larger sizes of the heavy alkalis exclude greater volumes in the pores of the zeolites.

Scanning electron micrographs of our zeolite materials are given in Fig. 1. The micron sizes of the faujasite-type zeolite particles shown in Figs. 1a and 1b are approximately an order of magnitude larger than the sizes of zeolites L and β particles shown in Figs. 1c and 1d. Ion exchange did not affect zeolite particle sizes.

The adsorption isotherms and t-plots for mesoporous alumina and cesium-impregnated (nominal 10 wt%) mesoporous alumina are shown in Fig. 2. Even though

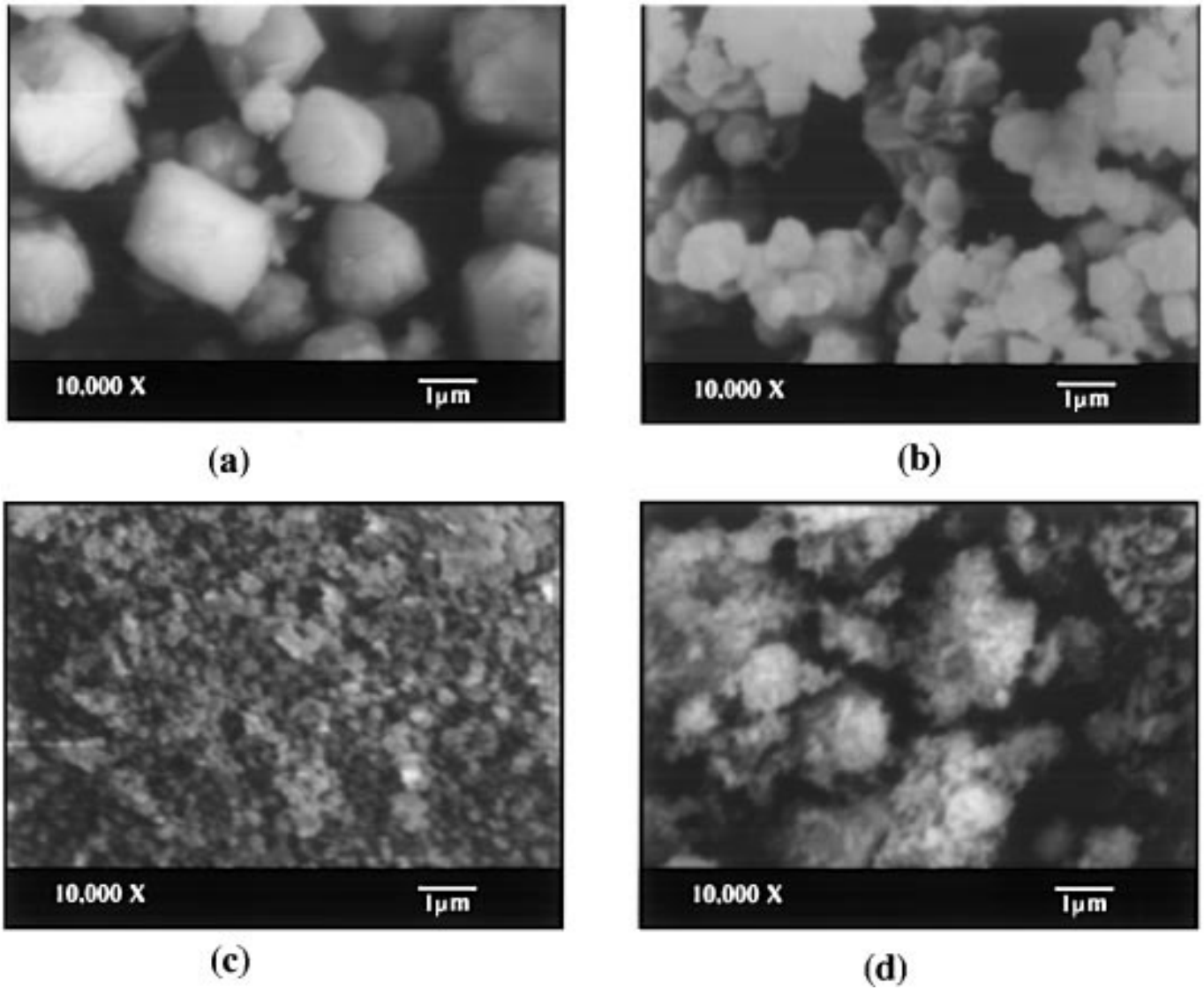

FIG. 1. Scanning electron micrographs of (a) zeolite X; (b) zeolite Y; (c) zeolite L; and (d) zeolite β.

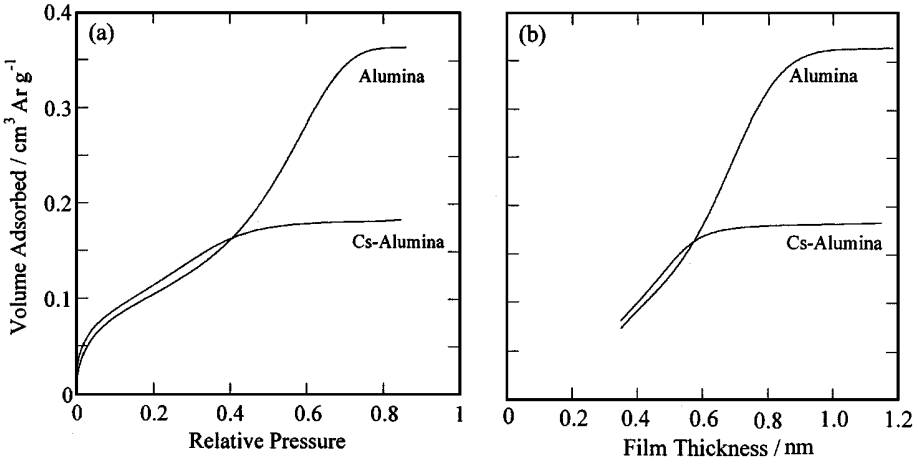

FIG. 2. Argon adsorption isotherms and t-plots of mesoporous alumina samples.

impregnation of cesium onto the alumina decreased the BET surface area from 370 to 315 $m^2\ g^{-1}$ and the total argon uptake by about a factor of 2, the t-plot analysis revealed that the Cs-alumina remained nonmicroporous. Vaudry *et al.* show similar results for a pure mesoporous alumina synthesized with lauric acid as a surfactant (17).

In an effort to probe zeolite basicity, carbon dioxide was irreversibly adsorbed at 373 K. Results from CO_2 adsorption on alkali-exchanged zeolites are listed in Table 2. The CO_2 uptakes for the X and Y zeolites are within 20% of each other, indicating that the materials have similar base site densities. Since basicity depends not only on the alkali cation but also on the percentage of alkali exchanged, it is not surprising that the adsorption capacities of X and Y zeolites were similar. Tsuji *et al.* also found that the CO_2 TPD curves for CsX, RbX, and KX were not significantly different (18). The most important result in Table 2 is that cesium-exchanged L and β zeolites adsorbed considerably less CO_2 than alkali-exchanged X and Y zeolites. The CO_2 uptake on CsL at 373 K was so low that we could not confidently report a value. Evidently, CsL and Csβ have far fewer basic sites than the CsX and CsY.

A complementary set of temperature-programmed desorption experiments was performed with an *in situ* IR cell. Carbon dioxide was adsorbed on alkali-modified zeolite wafers at 373 K for 20 min at a partial pressure of 0.5 atm in flowing helium. The samples were then purged for 60 min at 373 K to remove physisorbed and gas phase CO_2. The infrared spectra of adsorbed CO_2, with the contributions from the support subtracted, are shown in Fig. 3. Many researchers have found that carbonate species are formed by adsorption of CO_2 on zeolites and metal oxides (19–25). The IR spectra of the X zeolites in Fig. 3 are characteristic of bidentate carbonate with bands corresponding to both the ν^{as}_{C-O} and $\nu_{C=O}$ stretching modes. The carbonate species decomposed by 573 K for all samples except the CsX + B sample. Total desorption of CO_2 by 573 K on alkali-exchanged zeolite X was also observed by Tsuji *et al.* (18). Since the CO_2 adsorption capacities of CsX and CsY

TABLE 2

Carbon Dioxide Adsorption Capacities of Alkali-Exchanged Zeolites

Catalyst	Adsorbed CO_2/μmol g^{-1}
KX	134
CsX	118
CsY	119
Csβ	6
CsL	Trace

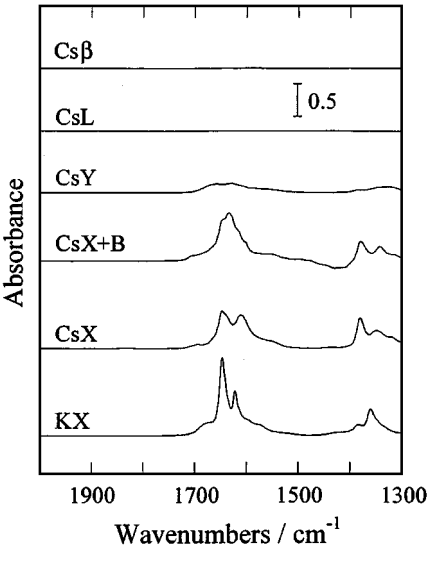

FIG. 3. Infrared spectra of CO_2 adsorbed on alkali-exchanged zeolites at 373 K. The zeolite has been subtracted.

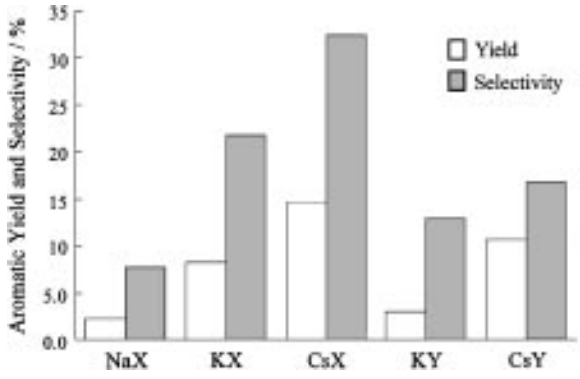

FIG. 4. Toluene alkylation over alkali-exchanged zeolites X and Y. Conditions: W/F: 20–30 g h $(mol)^{-1}$; T = 680–690 K; methanol conversion = yield/selectivity.

were about the same (Table 2), it is not immediately obvious why the peak intensities of CsY are less than those of CsX. Differences in the IR pellet thickness can partially account for the discrepency. No carbonate bands were observed in the spectra for CsL and Csβ, which confirmed the very low levels of CO_2 adsorption reported in Table 2 for these two samples.

Figure 4 summarizes the reactivity results for alkali-exchanged X and Y zeolites in the side-chain alkylation of toluene with methanol after approximately 2–4 h on stream. At constant temperature and W/F, the yield and selectivity to aromatics increased with increasing cation size. The NaX sample yielded small amounts of styrene and ethylbenzene and approximately two percent xylenes (not accounted for in Fig. 4). No xylenes were detected over any other catalyst. The presence of styrene and ethylbenzene, as well as xylenes, in the product stream from NaX indicates that both side-chain and aromatic ring alkylation can occur concurrently. Carbon monoxide was detected in significant quantities over all X and Y catalysts in Fig. 4, as indicated by the low selectivities to aromatics. After accounting for the formation of CO, the material balance on carbon closed to within five percent for those samples. Figure 4 also shows that the zeolite X materials were more reactive for base-catalyzed toluene alkylation than the analogous alkali-exchanged Y zeolites.

Earlier reports suggest that boron is an effective promoter for the base-catalyzed alkylation of toluene with methanol (6, 8, 14, 26–28). Boron probably moderates the strengths of the very strongest base sites which catalyze the undesirable decomposition of methanol to carbon monoxide. As shown in Fig. 5, impregnation of CsX with boric acid increased the yield and selectivity to styrene and ethylbenzene for loadings up to 0.8 wt%. The selectivity increased to greater than 70% by the further addition of boric acid. However, the increased selectivity was accomplished at the expense of decreased aromatic yield. These results must be interpreted with care since methanol conversions were not constant. Nevertheless, base sites active for alkylation appear to be neutralized with loadings of boric acid greater than about 0.8%.

Figure 6 shows the aromatic yield, selectivity, and methanol conversion at three different reaction temperatures for CsX + B, Csβ, and CsL catalysts. The CsX + B sample has a 1.2 wt% nominal loading of boric acid and has the highest selectivity to aromatics among our faujasite-type zeolites. Raising the reaction temperature from 690 to 760 K increased the yield to styrene and ethylbenzene over all the catalysts in Fig. 6. However, the selectivity of CsX + B decreased with increasing temperature due to excessive formation of carbon monoxide. The selectivity to aromatics was between 97 and 100% for the cesium-exchanged L and β zeolites because only trace quantities of carbon monoxide were detected. For these catalysts, the material balance based on carbon did not close satisfactorily and we suspected that formaldehyde was being produced instead of carbon monoxide. Since our gas chromatographic system could not reliably measure formaldehyde concentrations, we chose an alternate analysis technique. Condensation of the effluent stream in a dry ice–acetone cold trap followed by semiquantitative analysis of the condensate with calibrated formaldehyde test strips (Merck & Company) indicated that the amount of detected formaldehyde was appropriate to close the material balance. Figure 7 shows the product distributions for the catalysts in Fig. 6. Typical of our X and Y catalysts, the CsX + B zeolite produced only aromatics and carbon monoxide. In contrast, CsL and Csβ catalysts formed predominantly formaldehyde. Higher reaction temperatures simply increased the ratio of aromatics to formaldehyde. Recall that formaldehyde formed *in situ*

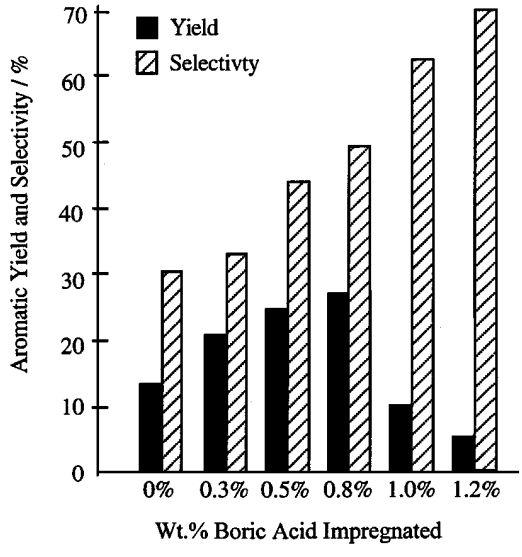

FIG. 5. Effect of boron on toluene alkylation over cesium-exchanged zeolite X. Conditions: W/F: 20–30 g h $(mol)^{-1}$; T = 680–690 K; methanol conversion = yield/selectivity.

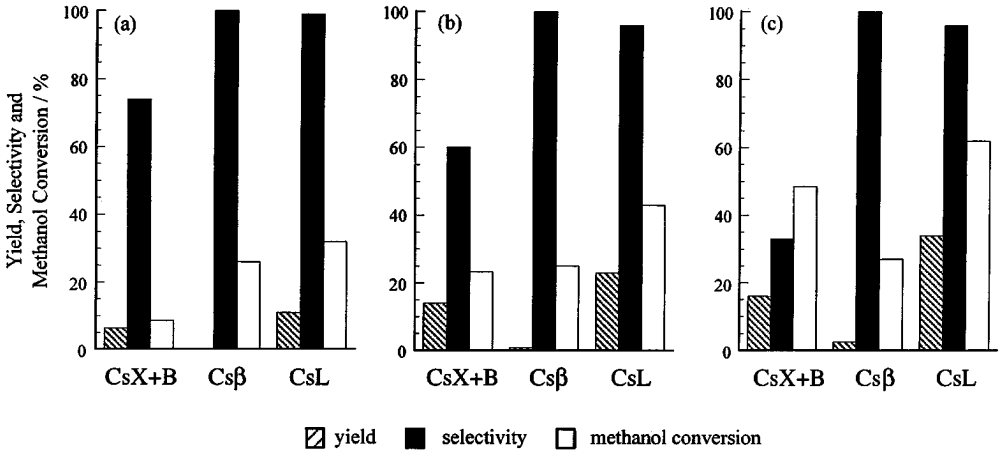

FIG. 6. Toluene alkylation over cesium-exchanged zeolites at (a) 690 K; (b) 725 K; and (c) 760 K. Conditions: W/F: 20–30 g h $(mol)^{-1}$; methanol conversion = yield/selectivity.

is considered to be the actual alkylating agent for this reaction (1, 11).

Figures 8 and 9 compare CsL to alkali-exchanged X and Y catalysts at various reaction conditions. As seen in Fig. 8, the aromatic yield from both CsX and CsL initially increased with W/F and reached a fairly constant plateau region. This trend is also seen with the other zeolite catalysts. The effect of reaction temperature on aromatic yield is shown in Fig. 9. The yield from CsL continuously increased up to the maximum temperature investigated. Temperatures greater than 800 K were not studied since methanol decomposed in the absence of catalyst. The aromatic yield over KY was only weakly affected by reaction temperature in the range reported in Fig. 9. In fact, there appears to be a maximum aromatic yield at an intermediate temperature. This behavior is typical of ion-exchanged X and Y zeolites. To attain aromatic yields comparable to our best CsX catalyst, CsL and Csβ required higher temperatures.

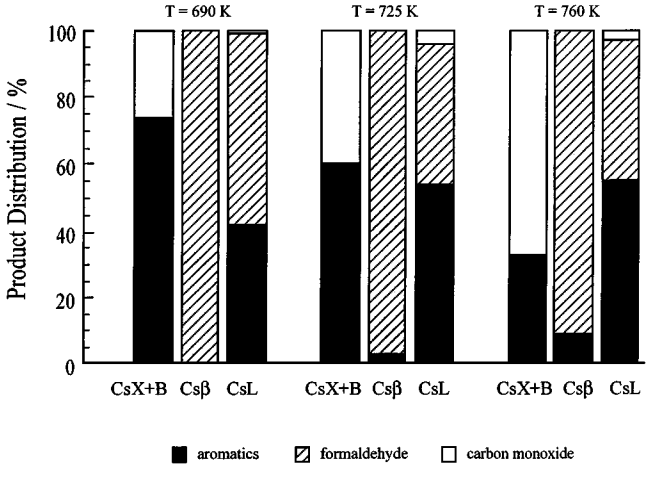

FIG. 7. Product distribution from toluene alkylation over cesium-exchanged zeolites at various temperatures with W/F = 20–30 g h $(mol)^{-1}$ at 690, 725, and 760 K.

Figure 1 shows that the highly selective L and β zeolites have much smaller particle sizes than either of the X or Y zeolites. To examine the role of particle size on the toluene alkylation reaction, a ball milled NaY zeolite (milled for 1 h) was exchanged with cesium and tested for catalytic activity. Figure 10 and Table 3 show the effects of ball milling time on crystallinity, pore volume, and particle size of NaY zeolite. Ball milling breaks apart zeolite particles and results in a total loss of crystallinity after extended treatment. Localized heat and pressure due to the grinding process are the most likely causes for the collapse in structure. We chose to study a sample that had been milled for 1 h since it exhibited smaller particle sizes than the unmilled material (see Fig. 11), yet retained some crystallinity. Figure 12 compares the reactivity of our standard CsY and ball milled

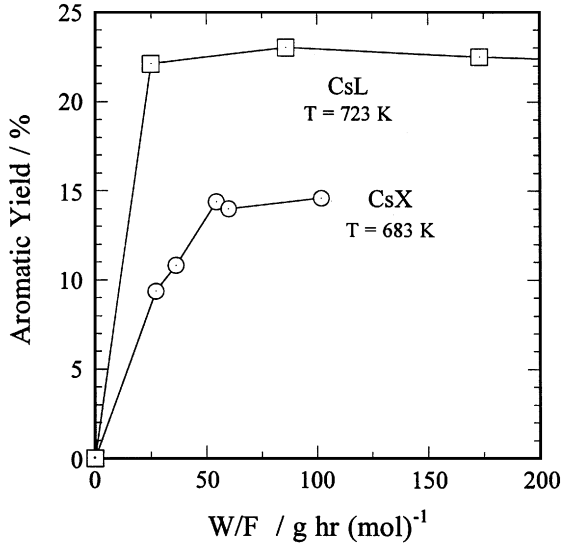

FIG. 8. Effect of W/F on toluene alkylation over Cs-exchanged X and L zeolites.

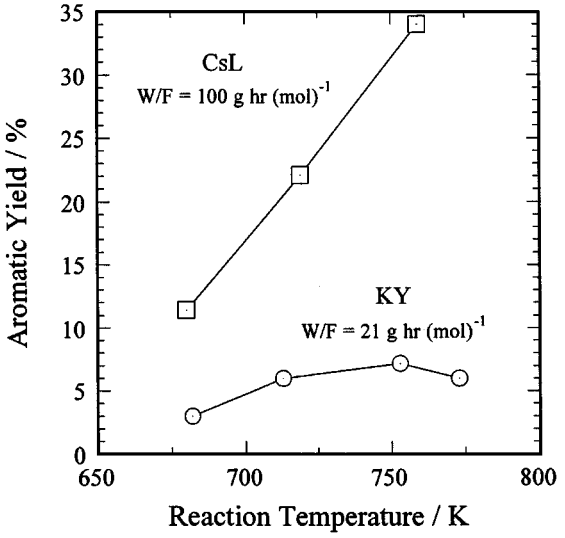

FIG. 9. Effect of temperature on toluene alkylation over CsL and KY zeolites.

CsY zeolites. Even though the ball milled sample was less active in terms of methanol conversion and aromatic yield, the selectivity to aromatics was the same as the standard material. These results show that smaller particle sizes did not prevent methanol decomposition to carbon monoxide.

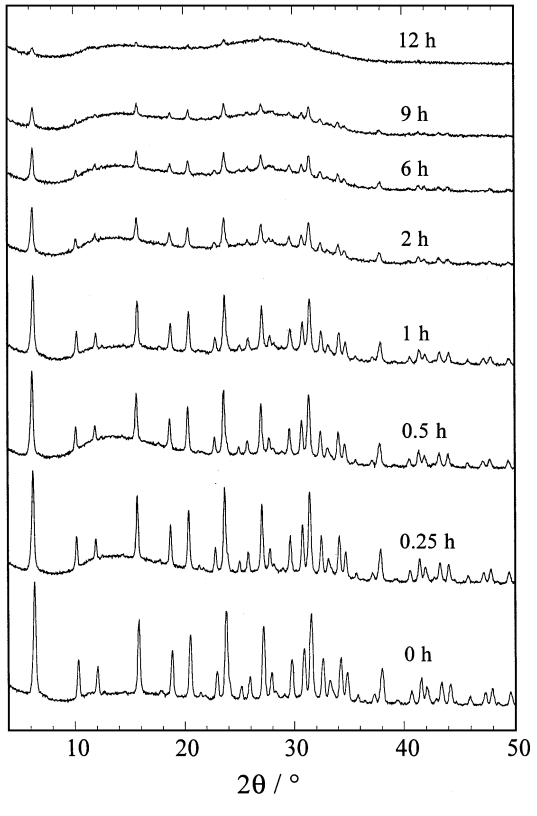

FIG. 10. X-ray diffractograms of ball milled NaY zeolites.

TABLE 3

Effects of Ball Milling on NaY

Catalyst	Pore volume/cm^3 Ar (g zeolite)$^{-1}$	Particle diameter/μm
NaY—as received	0.281	0.8–1.0
NaY—milled 15 min	0.210	0.6–1.0
NaY—milled 30 min	0.196	0.5–1.0
NaY—milled 1 h[a]	0.144	0.3–0.8
NaY—milled 2 h[a]	0.066	0.2–0.4
NaY—milled 6 h	0.057	0.2–0.3
NaY—milled 9 h	0.024	0.1–0.3

[a] Washed in hydroxide solution, used particulates which settled between 15 min and 6.5 h.

An exclusively mesoporous Al_2O_3 was also studied to determine if the physical constraints of a microporous environment were necessary for the side-chain alkylation of toluene. Table 4 summarizes the reactivity results for alumina impregnated with cesium (nominal loading of 10 wt%) and boric acid (nominal loading of 0.5 wt%). Addition of alkali to the inactive support created a highly basic material which led to nearly complete decomposition of methanol to carbon monoxide. Impregnation of boric acid onto $Cs–Al_2O_3$ neutralized some of the basic sites since methanol conversion was substantially lowered, but toluene alkylation was not observed.

DISCUSSION

The aromatic yield and selectivity for toluene alkylation with methanol over zeolites X and Y have been reported to increase with decreasing electronegativity of the exchanged cation (1, 2, 7–10, 14, 26, 28–32). The results in Table 1 and

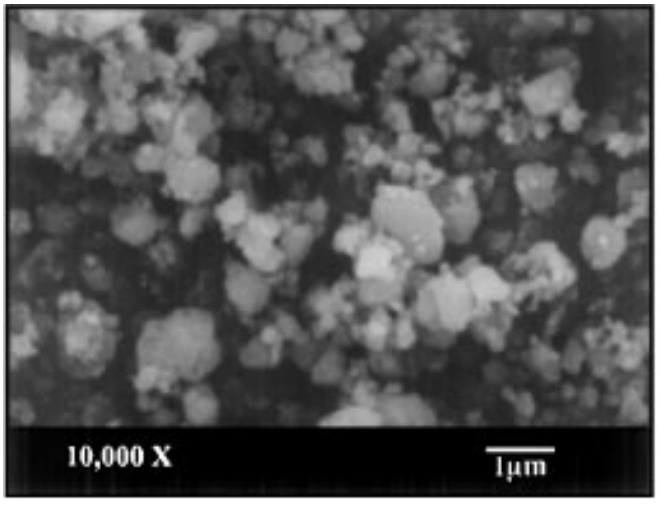

FIG. 11. Scanning electron micrograph of NaY that was ball milled for 1 h, washed, and settled.

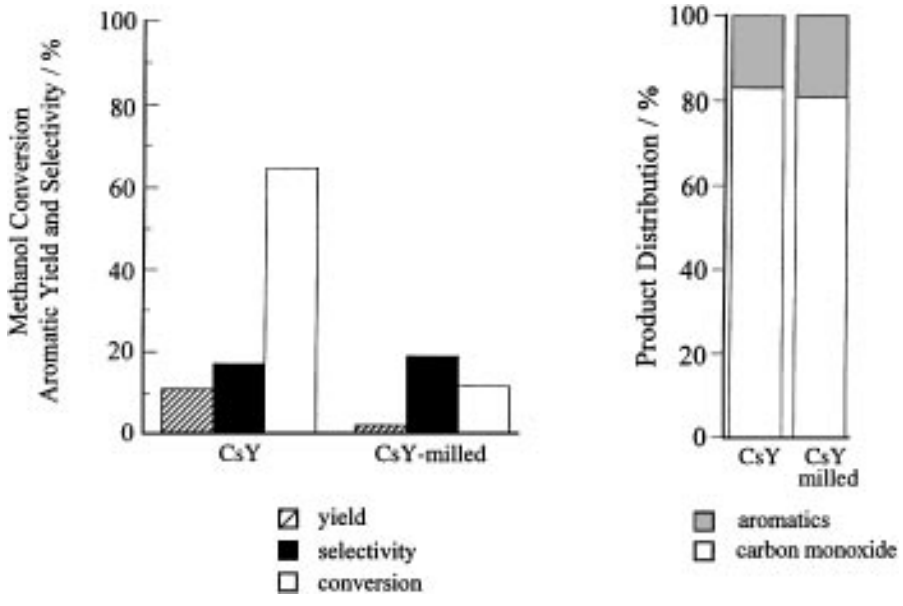

FIG. 12. Effect of ball milling (1 h) on toluene alkylation over Cs-exchanged zeolite Y. Conditions: W/F = 20–30 g h (mol)$^{-1}$; temperature = 680–690 K; methanol conversion = yield/selectivity; S = styrene; EB = ethylbenzene.

Fig. 4 demonstrate that our synthesis procedures and reaction protocols satisfactorily reproduce the trends found by others for the alkylation reaction over alkali-exchanged, faujasite-type zeolites. The major side product from reaction over basic X and Y zeolites is carbon monoxide derived from methanol decomposition.

The Cs-exchanged L and β zeolites also catalyzed the side-chain alkylation of toluene, but without substantial production of carbon monoxide. Instead, methanol decomposition was apparently halted at the intermediate product formaldehyde. Yashima *et al.* have shown experimentally that formaldehyde can alkylate toluene to produce styrene and ethylbenzene (2). Even though CsL was far more active than Csβ for alkylation, both catalysts are highly selective to formaldehyde, styrene and ethylbenzene.

Archier found that cesium-exchanged zeolite L was inactive for toluene alkylation (28). We also reported recently that a CsL material was ineffective for alkylation (26). However, we subsequently discovered that the crystallinity and catalytic behavior of ion exchanged L zeolites are sensitive to exchange conditions. The results presented in the current work clearly demonstrate that CsL can selectively catalyze toluene alkylation when the material is prepared properly. Similar conclusions can be drawn with regard to ion exchanged β zeolites.

The side-chain alkylation of toluene occurs in zeolites with one-, two-, and three-dimensional pore networks since the reaction is catalyzed by CsL, Csβ, and CsX (see Fig. 6). To the best of our knowledge, this is the first direct comparison of pore dimensionality on alkylation activity. Carbon supports with poorly defined micropore networks are also active catalysts for toluene alkylation after impregnation with Cs and B (14). Thus, it is not surprising that the pore dimensionality of a zeolite in not critical for alkylation activity.

Throughout the alkylation studies reported in the literature, most of the catalysts have been microporous (zeolites and carbon) with the exception of the work by Tanabe *et al.* (33). They reported minimal aromatic yield and selectivity over solid base materials such as MgO, MgO–TiO_2, and CaO–TiO_2. We prepared an exclusively mesoporous alumina to test the side-chain alkylation of toluene over a nonmicroporous solid. As summarized in Table 4, addition of alkali to mesoporous alumina created a basic material which led to the decomposition of methanol to carbon monoxide. Even after boron impregnation onto Cs-alumina, toluene alkylation was not observed. Since zeolites and microporous carbon are effective supports for Cs and B, whereas mesoporous alumina is not, pore size seems to play a significant role in toluene alkylation. However, more work is needed to elucidate the function of micropores in this

TABLE 4

Reaction of Toluene and Methanol over Mesoporous Alumina Catalysts

Catalyst	Methanol conversion/%	Selectivity to CO/%
Al_2O_3	0.0	0.0
Cs–Al_2O_3	97	100
Cs–Al_2O_3 + B	11	100

Note. Temperature = 683–693 K; W/F = 20–30 g h (mol)$^{-1}$.

reaction. For example, another reason basic alumina may not function effectively in toluene alkylation is the lack of cooperative Lewis acid/base pairs on the surface. Rubidium impregnated onto alumina is speculated to form a surface compound, most likely a rubidium aluminate (16). It is quite possible that this basic surface does not expose the proximal Lewis acid sites required to stabilize the aromatic ring of toluene.

The moderate levels of cesium incorporation in L and β zeolites, as indicated by elemental analysis, suggest that these materials should be basic. However, results from carbon dioxide adsorption and IR spectroscopy indicate that these zeolites have very few basic sites. In addition, only trace amounts of carbon monoxide were produced from these catalysts during toluene alkylation with methanol. Recall that methanol decomposition to carbon monoxide is significant over highly basic materials like CsX. Since CsL and Csβ zeolites contain less cesium than CsX and CsY zeolites, they are expected to have fewer base sites. Elegant work by Newell and Rees demonstrated that calcination of Cs-exchanged L zeolite causes migration of Cs ions from the main channels into locked positions behind the channel walls (34). Thus, the low basicity of our CsL sample may simply result from Cs migration after high temperature activation. Zeolite β is highly defective and may form Cs silicate with some of the incorporated alkali after thermal treatment. Doskocil *et al.* showed that impregnation of rubidium acetate onto pure silica gel followed by thermal decomposition of the acetate precursor produces a weakly basic surface rubidium silicate phase (16). The rubidium silicate adsorbed only trace quantities of CO_2 and was not an effective catalyst for 2-propanol dehydrogenation. Moreover, EXAFS studies revealed that the rubidium silicate is highly disordered. If some of the cesium in Csβ reacted with the silica component of the highly defective structure, a weakly basic compound could have formed.

The particle size of Y zeolite was decreased by ball milling in order to test the effect of diffusion path length. If the residence time of methanol inside the micropores of a zeolite crystal were critical to the decomposition reaction, then decreasing the crystal size should decrease carbon monoxide formation. Previous work on ball milling of zeolite Y suggests that basic sites are not significantly altered by a partial loss in crystallinity (35). Figure 12 shows that our ball milled zeolite was less active for both toluene alkylation and methanol decomposition, presumably a result of the partial loss of crystallinity. The selectivity to carbon monoxide, however, was unaffected by particle size in the range investigated. Apparently, the basicity of the catalyst is more important than particle size for determining selectivity of the alkylation reaction.

The Sanderson intermediate electronegativity, S_{int}, has been used to rank the basicity of zeolites (36). As the value of S_{int} decreases, the overall basicity of a material increases. Since the calculation of S_{int} is based on the overall composition of a solid, zeolites of various structures can be compared. Figure 13 summarizes the results from many previous studies of toluene alkylation by plotting the yield of aromatics as a function of Sanderson intermediate electronegativity of the zeolite catalysts (30, 37). As pointed out by others, acid-catalyzed alkylation of the aromatic ring to form xylenes (indicated by ○) occurs over materials having an intermediate electronegativity greater than about 3.6, whereas base-catalyzed alkylation of the methyl group to form styrene and ethylbenzene (indicated by ●) occurs over zeolites with an intermediate electronegativity less than about 3.6 (30, 37). The alkali-exchanged X and Y zeolites used in this study (indicated by □) follow the same trend as reported previously. The aromatic yields for our cesium-exchanged L and β zeolites at various reaction temperatures are also shown on Fig. 13 for comparison. Their elemental compositions place them in a region of the plot normally occupied by acid catalysts that produce xylenes. However, styrene and ethylbenzene are the only aromatic products formed over the CsL and Csβ catalysts. Since catalysts that produce xylenes normally contain acidic protons, a unique aspect of our work is that we have prepared zeolites with very few basic sites and no protonic sites. Thus, the alkylation of toluene is directed to the side-chain to produce styrene and ethylbenzene, but methanol is not decomposed to carbon monoxide. Simple extrapolation of the filled circles in Fig. 13 to lower electronegativities suggests that the aromatic yield would continue to increase with basicity. However, undesirable decomposition of methanol is likely to dominate the reaction. Our results suggest that materials with few basic sites are potentially useful toluene alkylation catalysts.

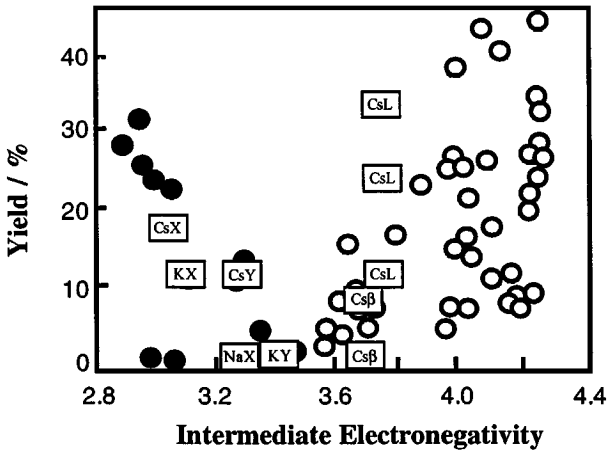

FIG. 13. Aromatic yield from toluene alkylation as a function of the Sanderson intermediate electronegativity of zeolite catalysts. Circles are from Giordano *et al.* (30) (● styrene and ethylbenzene; ○ xylenes) and squares are from this work.

CONCLUSIONS

Among X and Y zeolites, Cs-exchanged materials were the most effective catalysts for side-chain alkylation of toluene with methanol, but mostly decomposed methanol to carbon monoxide. Impregnation of CsX with about 0.8 wt% boric acid resulted in substantial promotion of alkylation activity and selectivity, presumably due to the partial neutralization of strongly basic sites that decompose methanol to carbon monoxide. Cesium-exchanged L and β zeolites also catalyzed the alkylation reaction, but with significant formation of formaldehyde instead of carbon monoxide. These zeolite particles were smaller in size and far less basic-than X and Y zeolites. Alkylation of toluene over a ball milled Y zeolite resulted in the same aromatic selectivity as an unmilled sample, which suggests that methanol decomposition to carbon monoxide is fairly independent of particle size in the range investigated. Therefore, observed differences in aromatic yields and selectivities among the materials studied here are attributed mostly to differences in basicity. Apparently, very few basic sites are needed to activate toluene in the presence of methanol without substantial production of CO. Extremely basic materials would not be effective catalysts due to excessive formation of carbon monoxide. Since zeolites with one-, two-, and three-dimensional pore networks are active alkylation catalysts, we conclude that pore dimensionality does not play a critical role in the reaction. Pore size and/or proximity of Lewis acid and base pairs, however, may be an important factor since a nonmicroporous Cs-impregnated alumina was found to be inactive for alkylation.

ACKNOWLEDGMENTS

This work was supported by a U.S. National Science Foundation Young Investigator Award (CTS-9257306) and the Dow Chemical Company. We thank Mr. Andrew Q. Campbell and Dr. Dean Millar from Dow Chemical Co. for synthesizing some of the catalyst samples.

REFERENCES

1. Sidorenko, Y. N., and Galich, P. N., *Dokl. Akad. Nauk, SSSR* **173**, 132 (1967).
2. Yashima, T., Sato, K., Hayasaka, T., and Hara, N., *J. Catal.* **26**, 303 (1972).
3. Philippou, A., and Anderson, M. W., *J. Amer. Chem. Soc.* **116**, 5774 (1994).
4. King, S. T., and Garces, J. M., *J. Catal.* **104**, 59 (1987).
5. Mielczarski, E., and Davis, M. E., *Ind. Eng. Chem. Res.* **29**, 1579 (1990).
6. Unland, M. L., and Barker, G. E., U.S. Patent 4,115,424 (1978).
7. Unland, M. L., and Barker, G. E., Catalysis of the toluene methanol reaction to form styrene and ethylbenzene, *in* "Catalysis of Organic Reactions" (W. R. Moser, Ed.), p. 51. Dekker, New York, 1981.
8. LaCroix, C., Deluzarche, A., Kiennemann, A., and Boyer, A., *Zeolites* **4**, 109 (1984).
9. Engelhardt, J., Szanyi, J., and Valyon, J., *J. Catal.* **107**, 296 (1987).
10. Hathaway, P. E., and Davis, M. E., *J. Catal.* **119**, 497 (1989).
11. Itoh, H., Miyamoto, A., and Murakami, Y., *J. Catal.* **64**, 284 (1980).
12. Itoh, H., Hattori, T., Suzuki, K., and Murakami, Y., *J. Catal.* **79**, 21 (1983).
13. Palomares, A. E., Eder-Mirth, G., and Lercher, J. A., *J. Catal.* **168**, 442 (1997).
14. Garces, J. M., Vrieland, G. E., Bates, S. I., and Scheidt, F. M., Basic molecular sieve catalysis: Side chain alkylation of toluene with methanol, *in* "Catalysis by Acids and Bases" (B. Imelik *et al.*, Eds.), p. 67. Elsevier Science, Amsterdam. 1985.
15. Wang, X., Wang, G., Shen, D., Fu, C., and Wei, M., *Zeolites* **11**, 254 (1991).
16. Doskocil, E. J., Bordawekar, S. V., and Davis, R. J., *J. Catal.* **169**, 327 (1997).
17. Vaudry, F., Khodabandeh, S., and Davis, M. E., *Chem. Mater.* **8**, 1451 (1996).
18. Tsuji, H., Yagi, F., and Hattori, H., *Chem. Lett.* 1881 (1991).
19. Angell, C. L., and Schaffer, P. C., *J. Phys. Chem.* **70**, 1413 (1966).
20. Bertsch, L., and Habgood, H. W., *J. Phys. Chem.* **67**, 1621 (1963).
21. Forster, M., and Schumann, M., *J. Chem. Soc., Faraday Trans.* **85**, 1149 (1989).
22. Hair, M., "Infrared Spectroscopy in Surface Chemistry," Dekker, New York, 1967.
23. Lercher, J. A., Colombier, C., and Noller, H., *J. Chem. Soc., Faraday Trans. I* **80**, 949 (1984).
24. Lavalley, J. C., *Catal. Today* **27**, 377 (1996).
25. Zecchina, A., Coluccia, S., Guglielminotti, E., and Ghiotti, G., *J. Phys. Chem.* **75**, 2790 (1971).
26. Wieland, W. S., Davis, R. J., and Garces, J. M., *Catal. Today* **28**, 443 (1996).
27. Unland, M. L., *J. Phys. Chem.* **82**, 580 (1978).
28. Archier, D., *Alkylation du Toluene par le Methanol en Ethylbenzene et Stryrene sur Zeolithes*, Claud Bernard-Lyon I, 1989.
29. Beltrame, P., Fumagalli, P., and Zuretti, G., *Ind. Eng. Chem. Res.* **32**, 26 (1993).
30. Giordano, N., Pino, L., Cavallaro, S., Vitarelli, P., and Rao, B. S., *Zeolites* **7**, 131 (1987).
31. Sidorenko, Y. N., and Galich, P. N., *Petroleum Chem.* **31**, 57 (1991).
32. Vasiliev, A. N., and Galinsky, A. A., *React. Kinet. Catal. Lett.* **51**, 253 (1993).
33. Tanabe, K., Takahashi, O., and Hattori, H., *React. Kinet. Catal. Lett.* **7**, 347 (1977).
34. Newell, P. A., and Rees, L. V. C., *Zeolites* **3**, 22 (1983).
35. Huang, M., Kaliaguine, S., and Auroux, A., *J. Phys. Chem.* **99**, 9952 (1995).
36. Mortier, W. J., *J. Catal.* **55**, 138 (1978).
37. Barthomeuf, D., *Catal. Rev.* **38**, 521 (1996).